

crinkle, a Novel Symbiotic Mutant That Affects the Infection Thread Growth and Alters the Root Hair, Trichome, and Seed Development in *Lotus japonicus*¹

Myra L. Tansengco, Makoto Hayashi*, Masayoshi Kawaguchi, Haruko Imaizumi-Anraku, and Yoshikatsu Murooka

Osaka University, Graduate School of Engineering, Department of Biotechnology, Yamadaoka 2-1, Suita, Osaka 565-0871, Japan (M.L.T., M.H., Y.M.); Niigata University, Faculty of Science, Department of Environmental Sciences, Ninomachi 8050, Ikarashi, Niigata City, Japan (M.K.); and National Institute of Agrobiological Sciences, Kannondai 2-1-2, Tsukuba, Ibaraki 305-8602, Japan (H.I.-A.)

To elucidate the mechanisms involved in *Rhizobium*-legume symbiosis, we examined a novel symbiotic mutant, *crinkle* (*LjSYM79*), from the model legume *Lotus japonicus*. On nitrogen-starved medium, *crinkle* mutants inoculated with the symbiont bacterium *Mesorhizobium loti* MAFF 303099 showed severe nitrogen deficiency symptoms. This mutant was characterized by the production of many bumps and small, white, uninfected nodule-like structures. Few nodules were pale-pink and irregularly shaped with nitrogen-fixing bacteroids and expressing leghemoglobin mRNA. Morphological analysis of infected roots showed that nodulation in *crinkle* mutants is blocked at the stage of the infection process. Confocal microscopy and histological examination of *crinkle* nodules revealed that infection threads were arrested upon penetrating the epidermal cells. Starch accumulation in uninfected cells and undeveloped vascular bundles were also noted in *crinkle* nodules. Results suggest that the *Crinkle* gene controls the infection process that is crucial during the early stage of nodule organogenesis. Aside from the symbiotic phenotypes, *crinkle* mutants also developed morphological alterations, such as crinkly or wavy trichomes, short seedpods with aborted embryos, and swollen root hairs. *crinkle* is therefore required for symbiotic nodule development and for other aspects of plant development.

The *Rhizobium*-legume interaction is one of the best-studied systems for approaching symbiotic functions and genes. The use of model legumes not only presents an attractive experimental basis for the study of nitrogen fixation and other areas of plant biology, but also provides opportunities for agronomic research (Cook et al., 1997). The features of *Lotus japonicus*, a representative plant for the determinate-type nodulation, have been extensively reviewed (Handberg and Stougaard, 1992; Jiang and Gresshoff, 1997). Legume nodulation involves several specific developmental steps and requires a coordinated expression of genes from both symbiotic partners. A valuable tool for understanding the nodulation process at the molecular level is the characterization of symbiotic mutants. In *L. japonicus*, detailed analyses of nodule organogenesis have been reported (Szczyglowski et al., 1998; Hayashi et al., 2000; van Spronsen et al., 2001) that provide the basic framework for the evaluation of nodulation mutants.

To date, several *L. japonicus* mutants with altered nodule phenotypes have been isolated and characterized (Imaizumi-Anraku et al., 1997; Schauser et al., 1998; Szczyglowski et al., 1998; Bonfante et al., 2000; Wopereis et al., 2000; Kawaguchi et al., 2002), but few symbiotic genes have been cloned. The *L. japonicus* nodule inception (*Nin*) gene, identified using a transposon-tagged symbiotic mutant, was the first plant gene responsible for nodule formation to be isolated (Schauser et al., 1999). Stracke and colleagues (2002) identified the *L. japonicus* SYMRK (for symbiosis receptor-like kinase) that is involved in recognizing microbial signal molecules. A similar receptor protein, NORK (for nodulation receptor kinase), was cloned in alfalfa (*Medicago sativa*) that is essential for Nod-factor signal perception and transduction (Endre et al., 2002). The *L. japonicus* ASTRAY (Nishimura et al., 2002b) and HAR1 gene products were recently identified that regulate the number of nodules (Krusell et al., 2002; Nishimura et al., 2002a). With the recent development of genetic and genomic tools for *L. japonicus*, other symbiotic genes are expected to be cloned that will help us understand the complex sequences involved in nodule organogenesis.

Screening of ethylmethane sulfonate (EMS)-mutagenized population of *L. japonicus* Gifu accession number B-129 yielded a variety of symbiotic mutants with phenotypes that are non-nodulating (Nod⁻), ineffectively nodulating (Fix⁻), or hyper-

¹ This work was supported by grants from the Ministry of Education, Culture, Sports and Technology of Japan (to M.L.T.), and the Core Research for Evolutional Science and Technology (CREST) from Japan Science and Technology Corporation (to M.H. and M.K.).

* Corresponding author; e-mail hayashi@bio.eng.osaka-u.ac.jp; fax 81-6-6879-7418.

Article, publication date, and citation information can be found at www.plantphysiol.org/cgi/doi/10.1104/pp.102.017020.

nodulating (Nod²⁺; Imaizumi-Anraku et al., 1997; Szczyglowski et al., 1998; Kawaguchi et al., 2002). In a recent report, ineffectively nodulating (Fix⁻) mutants were divided into two groups: the histogenesis⁻ (Hist⁻) and the Fix⁻ mutants (Kawaguchi et al., 2002). Hist⁻ involves the infection process with a defect in "cooperative histogenesis." Hist⁻ mutants produce nodule-like structures that are defective in tissue differentiation, such as nodule vascular bundles and bacterial infection zone. In contrast, Fix⁻ involves the functional process exhibiting symbiotic nitrogen fixation and includes mutants with ineffective nodules irrespective of the presence of many infected cells (Kawaguchi et al., 2002). *alb1* (*LjSYM74*) and *LjSYM79* mutants are categorized as Hist⁻ mutants. The *alb1* (for aberrant localization of bacteria inside the nodule) mutant was previously described (Imaizumi-Anraku et al., 1997, 2000) as having ineffective nodules in which bacteria remain in abnormally enlarged infection threads and fail to enter the host plant cells. In this mutant, incomplete development of vascular bundles is accompanied by very low or no expression of *ENOD40* (Imaizumi-Anraku et al., 2000). The nodule phenotype of *alb1* mutants shows that the *Alb1* gene is essential for normal development of the infection thread and for the initial stages of bacterial release from the infection thread.

Phenotypic characterization of other symbiotic mutants will identify specific stages of developmental arrest and will therefore indicate the function of the mutated genes. The infection thread is one of the morphological structures unique to the *Rhizobium*-legume symbiosis. Initiation and subsequent development of infection threads are crucial for the establishment of nitrogen-fixing nodules. Here, we present the symbiotic and non-symbiotic features of *LjSYM79*. We have called this mutant *crinkle* based on its obvious, aboveground non-symbiotic phenotype, crinkly or wavy trichomes. We show that abnormal nodulation in *crinkle* is caused by arrested infection threads at the epidermis. The pleiotropic nature of this mutant suggests that the *Crinkle* gene is required not only for infection thread development, but also for normal growth in other aspects of plant development.

RESULTS

Growth Inhibition of *crinkle* Is Caused by Limited Nitrogen Supply

Typical nitrogen deficiency symptoms were observed in *crinkle* mutants grown under nitrogen-starved conditions. In the absence of rhizobia and in the presence of low concentrations of nitrate (10 μ M), the overall growth of *crinkle* mutants was stunted compared with the wild-type Gifu. After inoculation with rhizobia, the mutant plants also exhibited a retarded growth. In a 10-d time course, significant

decrease in shoot growth and fewer lateral roots were observed in *crinkle* mutants (Fig. 1, A and C); however, no significant difference in root growth was noted between the wild-type and mutant plants (Fig. 1B). Prolonged infection with *Mesorhizobium loti* showed that 2-month-old *crinkle* plants were about one-half the size of wild-type plants of the same age (Fig. 2, A and B). The mutant roots were thinner and shorter than those of the wild type (Fig. 2, C and D; Table I). Also, shoots of *crinkle* mutants were chlorotic with small leaves and pigmented stems. The shoot growth of mutants 2 months after infection was significantly reduced by about 66% of the wild type (Table I). In the presence of a rich nitrogen source (10 mM KNO₃), *crinkle* growth was wild type (data not shown). This suggests that the abnormal growth of *crinkle* mutants was simply a result of limited nitrogen supply.

crinkle Mutation Alters Trichome, Seedpod, and Root Hair Development

Three non-symbiotic phenotypes were observed in the mutant plants. A remarkable characteristic of *crinkle* mutants was the abnormal trichome development. When observed under the microscope, trichomes of wild-type Gifu were straight (Fig. 3A), whereas those of *crinkle* were wavy or crinkly (Fig. 3B). This phenotype can be seen in the calyx, peduncle, rachis, stem, and midrib at the abaxial side of each leaflet. Another morphological alteration in *crinkle* mutants was the development of small seedpods. Mature pods of *crinkle* were about 43% shorter than in the wild type (Fig. 3, C and D; Table II); thus, *crinkle* mutants produced fewer seeds per pod. Aborted embryos, which appeared shrunken, thin, and small, were also observed more frequently in the mutant seedpods than in wild type (Fig. 3, E and F; Table II). Normal seeds of *crinkle* were slightly smaller than the wild-type seeds with an average weight of 0.74 and 0.98 mg seed⁻¹ ($n = 50$) for

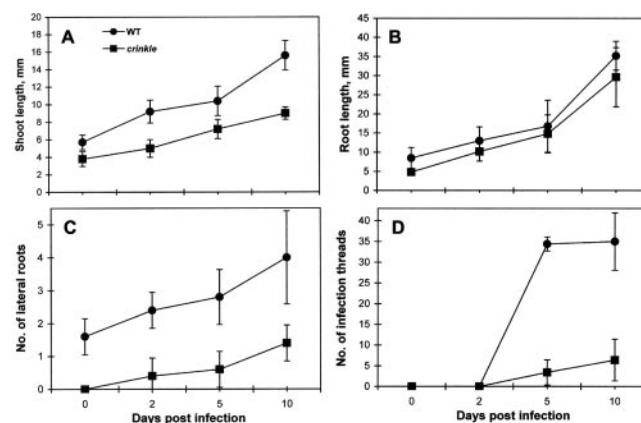
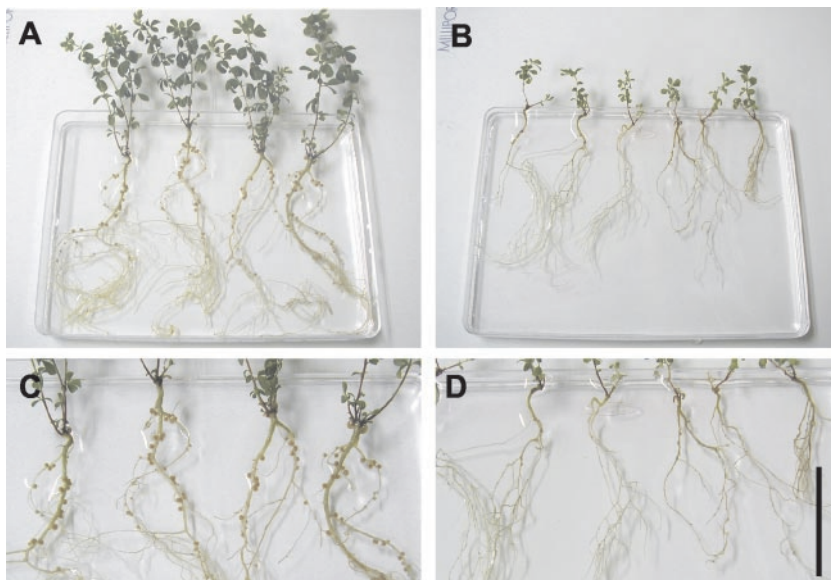


Figure 1. Growth kinetics of shoots, roots, lateral roots, and infection thread events in wild type and *crinkle* mutants. Five seedlings were examined at different intervals after inoculation with *M. loti*.

Figure 2. Growth and nodulation phenotypes of wild-type and *crinkle* plants 8 weeks after inoculation with *M. loti*. A, Normal growth of wild-type plants; B, *crinkle* mutants showing retarded growth and chlorotic leaves; C and D, Close-up of root sections shown in A and B, respectively. C, Pink nodules of wild type; D, abnormal nodulation in *crinkle*. Seedlings were grown in pillow system with Broughton and Dilworth medium supplemented with 10 μM KNO_3 . Bar = 5 cm.



mutant and wild type, respectively. The other non-symbiotic feature of *crinkle* mutants was the enlarged root hair base. In the absence of rhizobia, wild-type roots developed thin and straight root hairs, whereas *crinkle* formed root hairs swollen at the base (Fig. 4, A and B). In some root hairs of the mutant, the enlarged portion covered about one-half of the root hair cells. These non-symbiotic phenotypes of *crinkle* mutants were not affected by the presence of high concentration (10 mM) of nitrate (data not shown).

Infection Thread Development Is Arrested in *crinkle* Mutants

Root hair deformation assays showed that *crinkle* mutants exhibited delayed root hair responses to *M. loti* infection (Fig. 4D) as compared with wild type (Fig. 4C). After 1 to 5 d infection with *M. loti*, root hair deformations in *crinkle* mutants consisted largely of distal swellings (Fig. 4D). After longer infection, root hair distortion, shepherd's crooks, tip bending, and branching were also observed, as in the wild type (data not shown). Uninoculated control plants did not show any root hair response (Fig. 4, A and B).

To visualize bacterial infection in wild-type and mutant plants, derivatives of *M. loti* MAFF 303099, carrying *lacZ* or green fluorescent protein (GFP) reporter genes were used. Five and 10 d after infection with *M. loti* expressing GFP, very few root hairs of *crinkle* mutants were infected (Fig. 1D). Two weeks after inoculation, successful infection in the wild type allowed infection threads to penetrate the cortex and branch into fine networks (Fig. 5A). Infection thread networks in the developing nodule primordium can be observed within 1 week after inoculation with *M. loti*. In *crinkle* mutants, initiation and extension of infection threads in the root hairs appeared wild type; however, most ended in a balloon-shaped

structure at the base of the root hair cell, suggesting arrested penetration (Fig. 5B).

For β -galactosidase activity, roots were examined 8 d after infection with an *M. loti* strain carrying the *lacZ* reporter gene. In the wild type, bacterial invasion was evident by the presence of blue stains in the inner tissue of immature nodules (0.2–0.62 mm; Fig. 5C). Infection events not associated with nodule morphogenesis were arrested in the root epidermis without advancing beyond the stage of cortical cell divisions (data not shown). Examination of *crinkle* roots showed that immature nodules were smaller (0.06–0.25 mm) than the wild type and were associated with arrested infection events (Fig. 5D). Most of the infection threads in *crinkle* roots penetrated only the superficial layer of the bumps, indicating a halted infection progression in the nodule.

To confirm the specific cell layer in which infection threads of *crinkle* mutants arrest, roots were examined by confocal microscopy. In the wild type, successful infection was observed by the formation of an infection thread network in the developing nodules (Fig. 5E). In *crinkle* mutants, distinct infection threads were noted in the root hairs; however, infection

Table 1. Comparison of growth and nodulation between wild type and *crinkle*

Plants were grown in a pillow system and harvested 2 months after infection with *M. loti* MAFF 303099. Five plants were measured per sample, and means and sds are presented. White and pink nodules in *crinkle* mutants correspond to type I and type II nodules, respectively.

Parameters	Wild Type	<i>crinkle</i>
Root length (in mm)	95 \pm 5.55	79 \pm 13.88
Shoot length (in mm)	65 \pm 15.65	22 \pm 4.18
No. of pink nodules	39 \pm 3.57	4 \pm 0.71
No. of white nodules	0	38 \pm 5.07

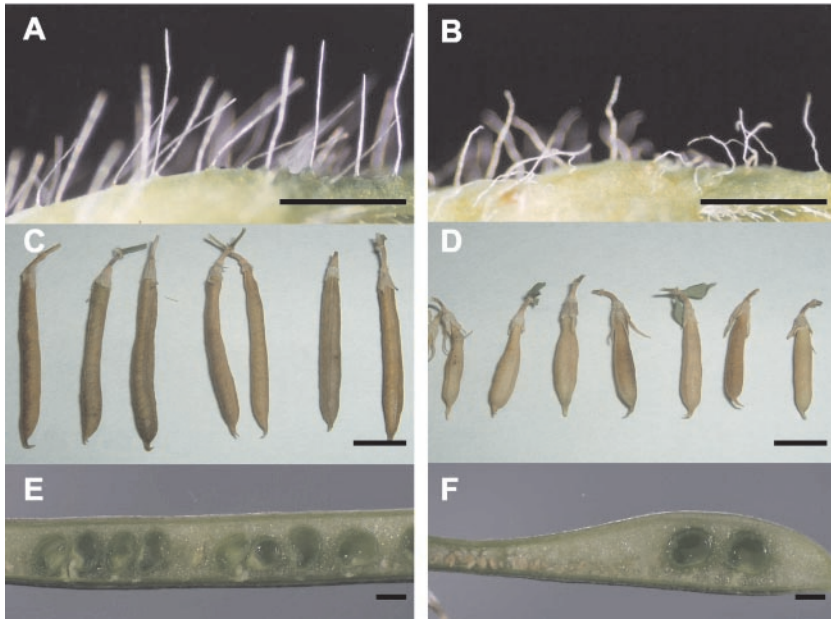


Figure 3. Morphological alterations of *crinkle* plants. A and B, Trichomes at calyx region. A, Straight trichomes of wild type; B, distorted trichomes of *crinkle*. C and D, Mature seedpods. C, Normal pods of wild type; D, short pods of *crinkle*. E and F, Immature seedpods. E, Wild-type pod with normal embryos; F, *crinkle* pod with many aborted embryos. Bars in A, B, E and F = 1 mm; and in C and D = 5 mm.

threads failed to enter the nodule cortical cells and were arrested at the epidermis (Fig. 5F).

crinkle Mutants Form Two Types of Nodules

Wild-type nodules induced by the infection of *M. loti* were spherical and pink at the nitrogen-fixing stage (Fig. 6A). The nodule primordia emerged within a few days after infection, and fully developed nodules were observed 1 week postinfection. In *crinkle*, abortion of infection threads resulted in the formation of many small bumps and white nodules (type I). Some enlarged, irregularly shaped, and pale-pink nodules (type II) also formed in the mutant roots (Fig. 6B). Two months after infection with rhizobia, wild-type plants consisted mainly of pink nodules (0.6–1.6 mm) that were infected (Table I; Fig. 6, A and C). *Crinkle* mutants developed mostly uninfected type I nodules (0.5–0.7 mm) and few infected type II nodules (1–1.8 mm; Table I; Fig. 6, B and D).

Histological examinations were performed to observe the detail structures of the nodules. In the wild type, 2 weeks after infection, a thick infection thread was noted at the epidermis that penetrated into the cortex (Fig. 7A). In this tubular infection thread, several vegetative bacteria were enclosed in the probably plant-derived infection thread wall. Many infected cells were also evident in the inner tissue of the nodule. In the mutant bump sections, bacteria were able to enter the curled root hair and initiate infection threads; however, infection thread penetration in the nodule primordium was not observed (Fig. 7, B and C). In addition, some root cortical cells in *crinkle* bump developed brownish pigmentation just near the infection sites (Fig. 7B). Such pigmented cells were rarely found in inoculated wild-type plants.

One month after infection, wild-type mature nodules primarily contained bacteroid-infected cells in the central zone with prominent vacuoles; in contrast, no infected cells were observed in the type I nodules of *crinkle* mutants (Fig. 7D). Instead, clumps of bacteria were noted in the outer cortex and in the central tissue of the nodules. These are bacteria that were not released from the infection thread, and they remained aggregated in the intercellular spaces. Autofluorescent walls were also observed surrounding those bacteria in the outer cortex (Fig. 7D). Examination of type II nodules of *crinkle* mutants showed some bacteroid-infected cells that were scattered in the central tissue (Fig. 7E). In *alb1-1* mutants, abnormal infection was characterized by the formation of a hypertrophied infection thread occupying a wide portion of the nodule central tissue (Fig. 7F).

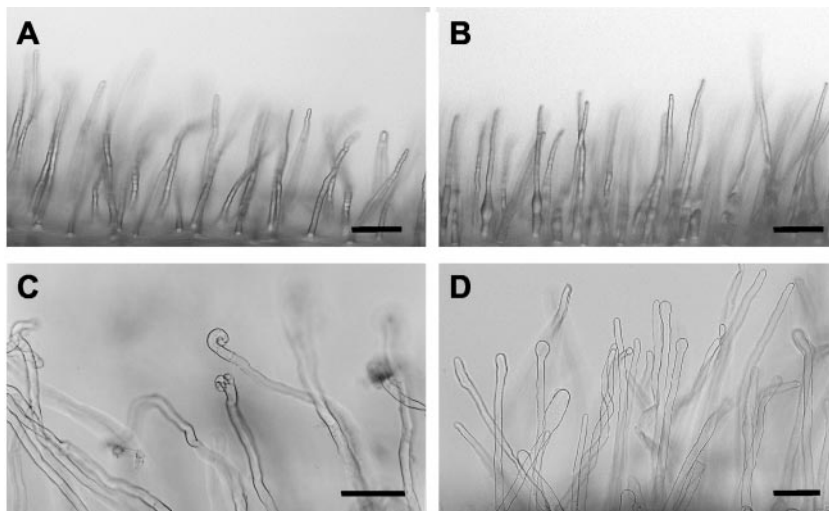
Periodic Acid-Schiff staining of wild-type nodules revealed few amyloplasts in the uninfected inner cortical cells, suggesting that transported photosynthates were metabolized (Fig. 8A). In both the empty (type I) and infected (type II) nodules of *crinkle* mutants, heavy accumulation of amyloplasts was ob-

Table II. Seeds and seedpod length of wild type and *crinkle*

Thirty mature seedpods were examined per sample, and means and SDs are presented. Aborted seeds refer to undeveloped embryos that appeared small, thin, and deformed.

	No. of Seeds per Pod			Seedpod Length mm
	Total	Normal	Aborted	
Wild type	16.4 ± 3.64	92.3%	7.7%	28 ± 2.75
<i>Crinkle</i>	7.0 ± 2.65	78.0%	22.0%	16 ± 3.26

Figure 4. Root hair deformations in wild type and *crinkle* after 3 d infection with *M. loti* MAFF 303099. A and B, Uninoculated roots; C and D, inoculated roots. A, Straight root hairs of wild type; B, root hairs of mutants with enlarged base; C, root hair deformations in wild type; D, tip swellings in *crinkle* in response to rhizobial infection. Bars in A and B = 100 μm ; in C = 50 μm ; and in D = 150 μm .



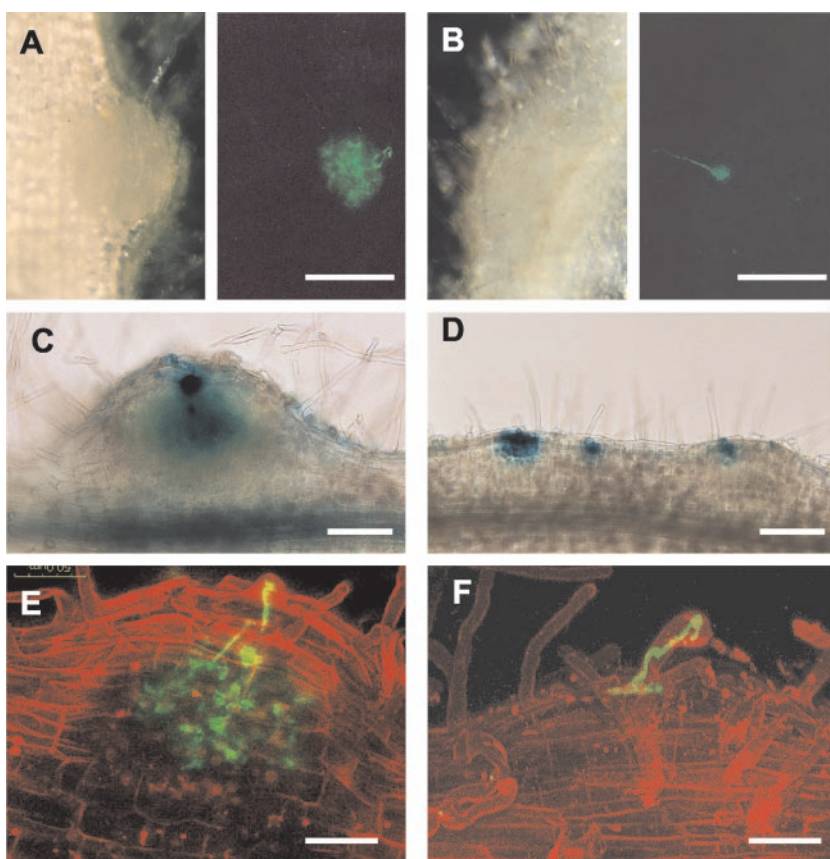
served (Fig. 8B). Undeveloped vascular bundles were also noted in *crinkle* nodules. In the wild type, vascular bundles bifurcate at the base of the nodule forming a network around the nodule periphery (Imaizumi-Anraku et al., 2000). In *crinkle*, although the vascular bundles branched, they failed to differentiate further. Thus, short and irregular vascular bundles developed in the proximal zone of *crinkle* nodules (data not shown). This undifferentiated vascular bundle phenotype resembles those of *alb1-1* mu-

tants (Imaizumi-Anraku et al., 2000) and was reported as a typical feature of Hist^- mutants (Kawaguchi et al., 2002).

Localization of Leghemoglobin Transcripts and Nitrogenase Activity in *crinkle* Nodules

Cellular localization of leghemoglobin mRNA in fully mature nodules of wild-type and *crinkle* plants was examined by in situ hybridization. In wild-type

Figure 5. Visualization of infection events in wild type and mutants after inoculation with *M. loti* carrying the GFP (A, B, E, and F) or *lacZ* gene (C and D). A and B, Light panels (left) represent micrographs of developing nodules by light microscopy, and adjacent dark panels (right) represent the same developing nodules viewed by fluorescence microscopy. A, Infection thread network in the wild-type nodule primordium; B, arrested infection in *crinkle* showing swelled infection thread at the base; C, successful infection in the wild type as indicated by the presence of blue stains in the inner tissue; D, arrested infections in *crinkle* at the superficial layer of the bumps. E and F, Confocal micrographs of root hairs with infection threads. Green represents GFP fluorescence, and red represents the fluorescence of the propidium iodide counterstain. E, Infection thread network in the wild type; F, arrested infection in *crinkle* at the epidermis. A and B, Two weeks after infection; C and D, 8 d after infection; E, 10 d after infection; and F, 15 d after infection. Bars in A and B = 250 μm ; in C and D = 150 μm ; and in E and F = 50 μm .



nodules, 2 months after infection, transcripts were detected in the infected cells of the central tissue (Fig. 8C). In *crinkle*, leghemoglobin expression was also detected in the few infected cells of type II nodules (Fig. 8D). No hybridization signal was observed when digoxigenin-labeled sense RNA transcripts were used as probes (data not shown).

Nitrogenase activity was determined to assess the ability of *crinkle* nodules to fix nitrogen (Table III). Three weeks after infection with *M. loti*, total nitrogenase activity (TNA) in *crinkle* nodules was relatively lower compared with those of wild-type and *alb1-1* plants. Four weeks after infection, TNA in *crinkle* was about one-half the activity of wild-type nodules; TNA in mutants then increased to 63% of wild-type levels after longer incubation (8 weeks after infection). We suspect that in *crinkle* mutants, detected nitrogenase activity corresponds to the emergence of some type II nodules several weeks after rhizobial infection.

DISCUSSION

Pleiotropic Phenotypes of *crinkle* Mutants

Here, we present the characteristics of *crinkle* mutants involved in both symbiotic and non-symbiotic processes. Mutation of this locus altered trichomes, seed development, and root hair cells (Figs. 3 and 4). Several pleiotropic nodulation mutants have been described previously, such as mutants *har1* (Wopereis et al., 2000) and *astray* (Nishimura et al., 2002b, 2002c) of *L. japonicus*, *sickle* of *Medicago truncatula* (Penmetza and Cook, 1997), and many symbiotic mutants of pea

(*Pisum sativum*; Guinel and LaRue, 1991; Lee and LaRue, 1992; Kneen et al., 1994; Guinel and Sloetjes, 2000). The nature of these mutants suggests that the nodulation process is integrated into the other aspects of plant development. The presence of aborted embryos in *crinkle* seedpods (Fig. 3F) might be correlated to the distorted segregation observed in the F₂ progeny from the cross between the mutant and wild-type Gifu (114:14; $\chi^2 = 13.5$; Kawaguchi et al., 2002). Szczygłowski et al. (1998) also identified three EMS-induced *L. japonicus* mutants that exhibit an unusual segregation ratio. These mutants were alleles *LjEMS45*, *LjEMS88*, and *LjEMS217*. Distorted segregation was reported as a common phenomenon in intra- and interspecies hybrids (De Martino et al., 2000). Its genetic basis may be the abortion of male or female gametes (Xu et al., 1997) or the selection process at the gamete or zygote stage (Gadish and Zamir, 1986; Zamir and Tadmor, 1986). Analysis of gametes and embryo development in *crinkle* will help us identify the cause of segregation distortion with this mutant. The aberrant trichome formation (Fig. 3B) and enlarged root hair base (Fig. 4B) of *crinkle* mutants might reflect a disturbed growth in these two related cell structures. Ringli et al. (2002) recently isolated and characterized the *der1* mutant, which is involved in root hair development. The *DER1* locus encodes ACTIN2 (ACT2), one of the two major actin genes expressed in vegetative tissue. Phenotypes of *der1* shows that ACT2 is not only involved in root hair tip growth, but is also required for correct selection of the bulge site on epidermal cell. Examination of the actin cytoskeleton and microtubule structure in *crinkle* mutants may reveal essential functions of the *Crinkle* gene in plant cell development.

Crinkle Is Involved in the Normal Infection Thread Development

Infection thread penetration from root hair cells to cortical cells is an important step leading to the establishment of legume-*Rhizobium* symbiosis. *M. loti* infections in *crinkle* were arrested upon reaching the base of epidermis (Fig. 5F); thus, many small, white, uninfected nodules were formed instead of infected nodules (Fig. 6B). Several symbiotic mutants arrested at the epidermis and at the cortex were described in pea (Guinel and LaRue, 1991; Geurts et al., 1997; Guinel and Sloetjes, 2000; Tsyganov et al., 2002). In a study with *Sinorhizobium meliloti* interactions with alfalfa, Ardourel et al. (1994) hypothesized that there are at least two Nod factor receptors in the epidermis: a signaling receptor and an entry receptor. The proposed entry receptor recognizes only Nod factors with appropriate decorations and induces the formation of an infection site and initial ingestion of bacteria; the signaling receptor controls the infection thread growth and root hair deformation that is less selective in Nod factor structure. In another study

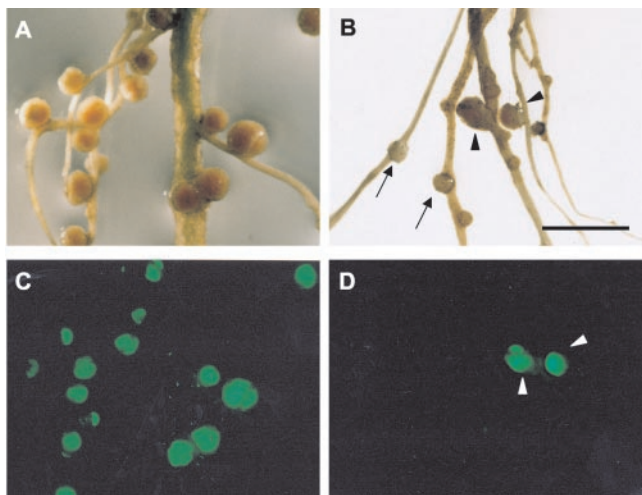
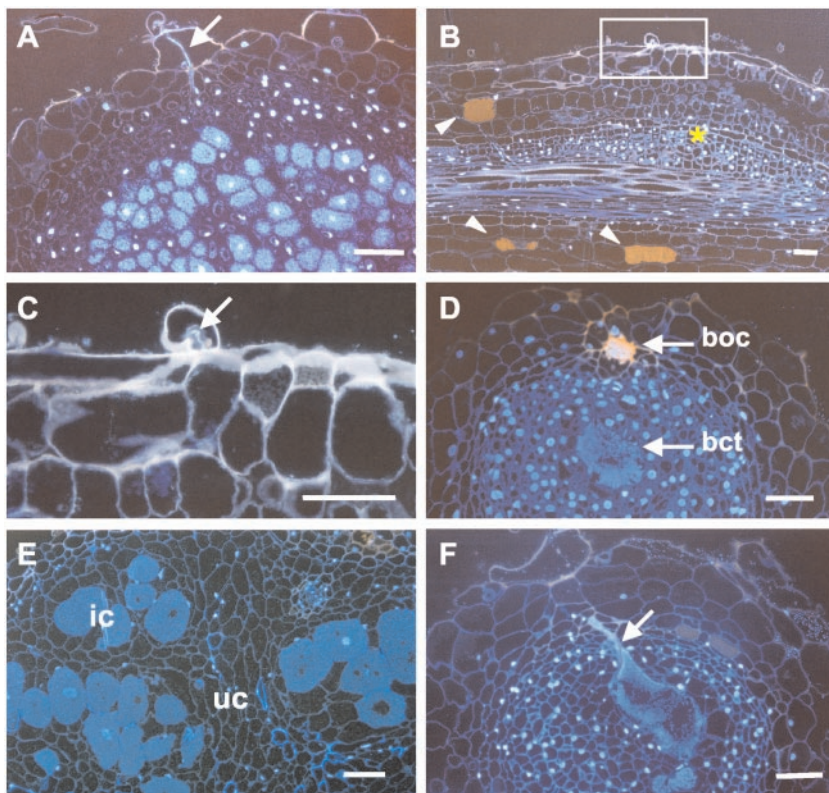


Figure 6. Nodulated roots of wild type and *crinkle* mutants 2 months after infection with *M. loti* strain carrying a GFP reporter gene. Light panels (top) represent micrographs of nodulated roots by light microscopy, and dark panels (bottom) represent the same nodulated roots viewed by fluorescence microscopy. A, Mature nodules of wild type; B, two types of nodules in *crinkle*. C and D, GFP expression in nodules shown in A and B, respectively. Arrow, Type I nodules; arrowhead, type II nodules. Bar = 3 mm.

Figure 7. Fluorescent micrographs of infection events in wild type and *crinkle* after 2 weeks (A–C) and 1 month (D–F) infection with *M. loti*. A, Developing nodule of wild type showing the infection thread and infected cells; B, bump of *crinkle* with arrested infection; C, close-up of thin section indicated in B; D, empty nodule (type I) of mutant showing aggregated bacteria in the intercellular spaces at the outer cortex (boc) and at the central tissue (bct); E, type II nodule of mutant containing infected cells scattered in the central tissue; F, Enlarged infection thread in the *alb1-1* nodule. Arrows, Infection thread; asterisk, cortical cell division; arrowheads, pigmented cortical cells; ic, infected cells; uc, uninfected cells. Bars = 50 μ m.



with *Rhizobium leguminosarum* mutants, Walker and Downie (2000) showed the role of *nodO* in stimulating infection thread development in vetch (*Vicia sativa*) and pea. *R. leguminosarum* bv *viciae* *nodE nodO* double mutants developed abnormal infection phenotypes, including intracellular accumulation of bacteria at the base of root hairs, distended and enlarged infection threads, and reversed threads growing up root hairs. These results indicated that the most basic Nod factor structure can allow bacterial entry into the root hair and that *nodO* can promote subsequent infection thread development.

In symbiotic nodule formation, the infection process itself involves a series of events. Tsyganov et al. (1998) reclassified the phenotypic codes for infection thread development as follows: Iti, infection thread initiation; Ith, infection thread differentiation inside the root hair cell; Itr, infection thread differentiation inside the root cortex; Itn, infection thread differentiation inside the nodule tissues; and Idd, infection droplet differentiation. The mutation in *Crinkle* influences the infection thread growth in the epidermis through the root cortex. On the basis of the system of the proposed phenotypic codes (Tsyganov et al., 1998), *crinkle* can be defined between the Ith⁻ and Itr⁻ phenotypes.

Characteristics of *crinkle* Nodules

Blocked infection thread development led to the formation of two nodule types on *crinkle* roots after

inoculation with *M. loti* (Fig. 6B). This nodulation phenotype of *crinkle* mutants is similar to those described for *L. japonicus alb1-1* (Imaizumi-Anraku et al., 1997), *M. truncatula* TE7 (Benaben et al., 1995), and pea SGEFix⁻² (*sym33*) mutants (Tsyganov et al., 1998). *alb1-1* can be distinguished from *crinkle* by the presence of more bumps and the formation of hypertrophied infection threads. It is likely that the *L. japonicus* Hist⁻ mutants, *alb1* and *crinkle*, affect different but adjacent developmental stages of the infection process. Creation of double mutants will confirm the sequential functioning of these *L. japonicus* symbiotic genes. Starch accumulation in *crinkle* nodules (Fig. 8B) was also described in *L. japonicus alb1* and *fen1* (Imaizumi-Anraku et al., 1997) and in ineffective mutants of alfalfa (Vance and Johnson, 1983), soybean (*Glycine max*; Forrest et al., 1991), and pea (Novak et al., 1995). The presence of amyloplasts suggests that the plant-derived photosynthates, which serve as an energy source for nitrogen fixation, are not fully consumed in this type of nodule (Postma et al., 1990).

We observed host defense-like responses in *crinkle*, such as the presence of pigmented cortical cells near the infection sites (Fig. 7B) and autofluorescent walls surrounding the bacterial cells (Fig. 7D). In alfalfa, with its regular symbiont *Sinorhizobium meliloti*, Vasse et al. (1993) observed chemical modification of cell walls and accumulation of plant defense-related compounds in necrotic cells. The authors noted that this localized host defense response is part of the

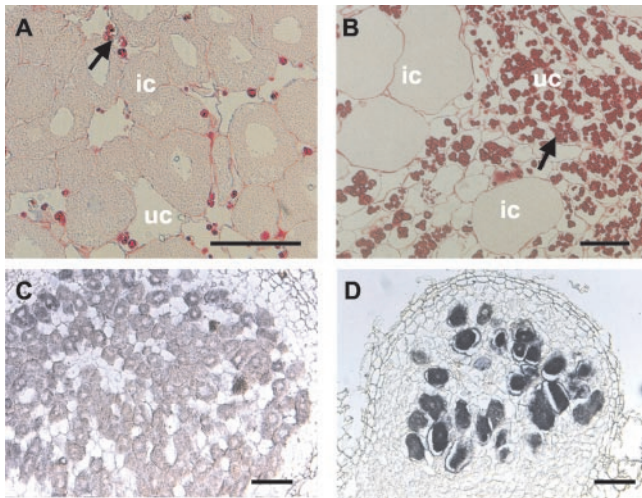


Figure 8. Amyloplast accumulation and in situ localization of leghemoglobin transcripts in nodules of wild-type and *crinkle* plants. A, Central zone of wild-type mature nodule with many infected cells. Few amyloplasts are present in the uninfected cells. B, Type II nodule of *crinkle* with some infected cells and with heavy accumulation of amyloplasts; C and D, longitudinal sections hybridized with anti-sense RNA probes showing leghemoglobin expression in the infected cells of wild type and *crinkle*, respectively. Arrows, Amyloplasts; ic, infected cells; uc, uninfected cells. Bars in A and B = 50 μm ; and in C and D = 100 μm .

autoregulatory mechanisms to control nodule formation (Vasse et al., 1993). In SGEFix⁻¹ (*sym40*) and SGEFix⁻² (*sym33*) of pea, host defense reactions are characterized by premature degradation of nodule tissue and “locked” infection threads surrounded by thick plant cell walls (Tsyganov et al., 1998). In the *M. truncatula* mutant TE7, accumulation of polyphenols in the cell walls of root cortex was also noted (Benaben et al., 1995). In *crinkle*, there is a possibility that the mutation might cause the activation of the host defense response during bacterial penetration; thus, progression of the infection thread from the epidermis to the cortex was inhibited. In other plant species, recessive mutations cause spontaneous cell death in leaves and roots associated with various symptoms of plant defense in the absence of pathogens (Dangl et al., 1996). It will be of interest to

Table III. Nitrogenase activity in the wild type, *crinkle*, and *alb1-1* nodules

Nitrogenase activity was determined in intact plants by H₂ evolution assay. Two nodulating plants were examined for each genotype, and means and sds are presented. N.D., Not determined.

	Total Nitrogenase Activity		
	3wpi	4wpi	8wpi
	$\mu\text{mol h}^{-1} \text{plant}^{-1} \pm \text{sd}$		
Wild type	9.44 \pm 6.26	16.84 \pm 3.29	19.29 \pm 5.09
<i>alb1-1</i>	8.48 \pm 6.34	12.12 \pm 3.35	N.D.
<i>crinkle</i>	3.03 \pm 4.07	8.49 \pm 1.06	12.19 \pm 9.62

determine whether the plant defense response is implicated in the *crinkle* phenotype.

In summary, our results suggest that abortion of infection thread at the epidermis is correlated with the abnormal nodulation in *crinkle* mutants. The mutual recognition between the host plant and rhizobia upon penetration of basal epidermis might be affected by mutation of the *crinkle* locus. We propose that the sequential functioning of characterized *L. japonicus* symbiotic genes controlling early nodule development is as follows: (*SYMRRK*, *LjSym4*) \rightarrow *Lj-Nin* \rightarrow *Crinkle* \rightarrow *Alb1* \rightarrow *Fen1*. The pleiotropic phenotypes of *crinkle* mutants are distinct from previously described ineffectively nodulating mutants of *L. japonicus* and of other legume species. Thus, *crinkle* may define a new locus involved in root nodule symbiosis and in other tissue development. Map-based cloning and analysis of *Crinkle* gene will help to uncover its function in the infection process during nodule development and in other aspects of plant biology.

MATERIALS AND METHODS

Plant Materials

The *crinkle* mutants were produced from EMS mutagenesis of *Lotus japonicus* Gifu accession number B-129 and were backcrossed twice with the wild-type Gifu before phenotypic analysis (Kawaguchi et al., 2002). Both wild-type Gifu and *crinkle* seeds were scarified for 10 min in concentrated sulfuric acid, rinsed three times under running water, and then surface sterilized with 10% (v/v) NaClO for 10 min. Treated seeds were washed three times with sterile water and were kept in sterile water for 2 to 3 h at room temperature. Seeds were germinated on 0.8% (w/v) Bacto agar in petri dishes and incubated in a growth cabinet under 16-h-light/26°C and 8-h-dark/23°C cycle with 60% relative humidity. The *alb1-1* mutants (*LjSym74-1*; Imaizumi-Anraku et al., 1997) were also used to compare their nodulation and histological structures with that of *crinkle* mutants.

Bacterial Strains

Mesorhizobium loti MAFF 303099 was obtained from the Ministry of Agriculture, Forestry and Fisheries, National Institute of Agrobiological Sciences, Japan. The *M. loti* BN02 mutant expressing eGFP was obtained from Dr. K. Saeki (Osaka University, Japan), and *M. loti* MAFF 303099 derivative ML001 carrying pDG499 (*nodB:lacZ*) constitutively expressing the β -galactosidase (*lacZ*) reporter gene was provided by Dr. K. Minamisawa (Tohoku University, Japan). Bacteria were grown at 28°C for 2 d in tryptone-yeast extract medium with 15 $\mu\text{g mL}^{-1}$ phosphomycin for *M. loti* MAFF 303099, 10 $\mu\text{g mL}^{-1}$ gentamycin for *M. loti* harboring the GFP gene, and 15 $\mu\text{g mL}^{-1}$ tetracycline for *M. loti* carrying the *lacZ* gene.

Root Hair Deformation Analysis

Root hair deformation assays were as described by Bonfante et al. (2000). Sterilized seeds were imbibed for 2 d on wet filter paper. Germinated seedlings were then transferred on one-fourth-strength Broughton and Dilworth agar medium. Plates were positioned vertically to facilitate straight root growth. Seedlings were grown for 2 d before infecting with *M. loti* MAFF 303099 at a cell density of 10⁸ cells mL⁻¹. Three days later, roots were harvested and cleared with 20% (v/v) sodium hypochlorite for a few minutes. Cleared samples were rinsed three times with water and examined under a light microscope (BX50, Olympus Optical Co., Tokyo).

Infection Thread Examination

To visualize infection threads, roots were inoculated with *M. loti* strain expressing either eGFP or *lacZ* reporter gene. Seedlings of 7-d-old wild type and *crinkle* mutants were transferred to the "pillow system" (see below). Two days later, plants were inoculated with *M. loti* strains at a density of 10^8 cells mL⁻¹. At least 10 seedlings were inspected per genotype at different days after inoculation. For β -galactosidase activity, whole roots were vacuum infiltrated for 3 min with fixative solution (1% [v/v] glutaraldehyde in 1× phosphate-buffered saline [PBS] buffer, pH 7.5) and incubated in PBS buffer for an additional 1 h. Fixed samples were subsequently washed twice with PBS buffer and stained for β -galactosidase activity using a solution composed of 0.2× PBS (pH 7.5), 2.5 mM K₃[Fe(CN)₆], 2.5 mM K₄[Fe(CN)₆], and 0.8 mg mL⁻¹ of 5-bromo-4-chloro-3-indolyl- β -D-galactoside (Nacalai Tesque, Inc., Kyoto) in *N,N*-dimethylformamide. Staining was done by vacuum infiltrating for 3 min and then incubating overnight at room temperature. Stained samples were rinsed three times with PBS and cleared in 20% (v/v) sodium hypochlorite solution. Infection threads were observed using an Olympus BX50 microscope under bright-field illumination (for *lacZ*) or under fluorescent attachment (for GFP).

For confocal microscopy of infection threads, roots were infected with *M. loti* expressing GFP. After 10 to 15 d inoculation, roots were cut and immersed in 10 μ g mL⁻¹ propidium iodide solution for 30 min to stain the cell wall (Gage et al., 1996). Tissues were then washed with sterile water. Confocal microscopy was done on an Olympus FV500 confocal laser scanning microscope as described by Gage et al. (1996).

Nodule Examination

Seven-day-old seedlings were transferred to a pillow system, as described previously by Szczygłowski et al. (1998) with some modifications. Polypropylene tea packs (120 × 95 mm) were used as pillow bags. A single pillow system was composed of 12 to 15 tea bags, placed side by side in a plastic tray (30 × 10 × 10 cm). Tea packs were filled with vermiculite:perlite (6:1, w/w) mixture and then soaked in Broughton and Dilworth nutrient solution containing 10 μ M KNO₃ for about 15 min. This low concentration of nitrate did not affect nodule formation of the inoculated *L. japonicus* plants (data not shown). Seedlings were placed between individual pillows (five plants per row). After 2 d, roots were inoculated with *M. loti* expressing GFP at a density of 10^8 cells mL⁻¹. Weekly observation of the mutant phenotype was done. Whole nodulated roots were examined under a stereomicroscope with fluorescent attachment (MZFLIII, Leica Microsystems Co., Tokyo).

Histological Examination of Nodules

For histological examination of wild-type and *crinkle* nodules, 3- to 4-mm-long root segments were vacuum infiltrated for 30 min in 4% (w/v) paraformaldehyde in 2 mM sodium cacodylate buffer (pH 7). After overnight incubation in fresh fixing solution at 4°C, root segments were dehydrated in ethanol series (30%, 50%, 70%, and 80% [v/v], 2 × 15 min for each step; 90%, 95%, and 99% [v/v], 2 × 5 min for each step; and 100% [v/v] for 1 h). Infiltration and embedding were done according to the protocol of Histo-Technik 7100 (Kulzer, Wehrheim, Germany). Semithin sections (1–1.5 μ m) were cut from root-embedded samples using a glass knife on an ultramicrotome (Leica Ultracut S). Sections were stained with a solution consisting of 10 μ g mL⁻¹ 4',6-diamidino-2-phenylindole in vectashield (Vector Laboratories, Inc., Burlingame, CA), and 5 μ g mL⁻¹ fluorescent brightener 28 (Sigma-Aldrich, St. Louis).

Accumulation of Amyloplast in Nodules

Observation of amyloplasts in the nodules was performed on semithin sections. Samples were stained with Periodic Acid-Schiff staining system (Sigma Diagnostics, St. Louis) according to the manufacturer's instruction and examined under a light microscope.

In Situ Localization of Leghemoglobin Transcripts

Expression of the leghemoglobin gene was examined by in situ hybridization, as described by Kouchi and Hata (1993). For preparing sense and

antisense RNA fragments of the leghemoglobin gene, a 0.32-kb cDNA fragment obtained by reverse transcriptase-PCR from *L. japonicus* nodule RNA was cloned into pGEM T-easy vector (Promega, Madison, WI). Linearization with *Nco*I or *Sal*I provided templates for Sp6 and T7 polymerases to generate sense and antisense RNA, respectively. For the reverse transcriptase-PCR amplification, two primers specific to leghemoglobin gene were synthesized. The probes were digoxigenin-labeled using the Sp6/T7 DIG RNA-labeling kit (Roche Diagnostics, Mannheim, Germany).

For tissue preparation, nodules harvested 2 months after infection with *M. loti* MAFF 303099 were fixed with 4% (w/v) paraformaldehyde in 1× PBS (pH 7.4). Nodules were dehydrated through an ethanol series and embedded in paraffin embedding medium (Paraplast Plus, Oxford Labware, St. Louis). Microtome sections of 10 μ m thick were placed on a glass slide coated with poly-L-Lys. Sections were hybridized to digoxigenin-labeled sense or antisense leghemoglobin RNA at 50°C for 16 h, and successive washings were performed. The hybridization signals were visualized using an antidigoxigenin-alkaline phosphatase conjugate with nitroblue tetrazolium salt and 5-bromo-4-chloro-3-indolyl phosphate toluidium salt (Roche Diagnostics). Sections were examined under a light microscope.

Nitrogenase Activity

Nitrogenase activity of intact plants was measured in situ as H₂ evolution (Herrmann et al., 2002; Smith et al., 2002). Wild-type and mutant plants were grown in pots containing vermiculite:perlite mix (6:1, w/w). Three to 8 weeks after infection with *M. loti* MAFF 303099, nitrogenase activity was determined by passing the gas streams exiting the pots through an in-line H₂ detector (Qubit Systems Inc., Kingston, Ontario, Canada). The output from the H₂ detector was fed to a Universal Lab Interface and analyzed using the Logger Pro software (Vernier Software, Portland, OR). For the determination of apparent nitrogenase activity, the gas consisted of 80:20 (v/v) mixture of N₂:O₂ until stabilization was reached. The peak value observed after switching to 80:20 (v/v) mixture of Ar:O₂ was used to determine TNA. Nitrogen fixation rates were calculated by the following equation: (TNA – apparent nitrogenase activity)/3.

ACKNOWLEDGMENTS

We thank Dr. K. Saeki (Osaka University, Japan) and Dr. K. Minamisawa (Tohoku University, Japan) for providing the *M. loti* strains harboring the eGFP and *lacZ* reporter genes, respectively. We also thank Dr. Jeanne M. Harris (University of Vermont, Burlington) for her critical reading of the manuscript.

Received November 1, 2002; returned for revision November 24, 2002; accepted January 8, 2003.

LITERATURE CITED

- Ardourel M, Demont N, Debelle F, Maillet F, de Billy F, Prome JC, Denarie J, Truchet G (1994) *Rhizobium meliloti* lipooligosaccharide nodulation factors: different structural requirements for bacterial entry into target root hair cells and induction of symbiotic developmental responses. *Plant Cell* 6: 1357–1374
- Benaben V, Duc G, Lefebvre V, Huguet T (1995) TE7, An inefficient symbiotic mutant of *Medicago truncatula* Gaertn. cv Jemalong. *Plant Physiol* 107: 53–62
- Bonfante P, Genre A, Faccio A, Martini I, Schauser L, Stougaard J, Webb J, Parniske M (2000) The *Lotus japonicus* *LjSym4* gene is required for the successful symbiotic infection of root epidermal cells. *Mol Plant-Microbe Interact* 13: 1109–1120
- Cook DR, VandenBosch K, de Bruijn FJ, Huguet T (1997) Model legumes get the Nod. *Plant Cell* 9: 275–281
- Dangl JL, Dietrich RA, Richberg MH (1996) Death don't have no mercy: cell death programs in plant-microbe interactions. *Plant Cell* 8: 1793–1807
- De Martino T, Errico A, Lassandro A, Conicella C (2000) Distorted segregation resulting from pea chromosome reconstructions with alien segments from *Pisum fulvum*. *J Hered* 91: 322–325
- Andre G, Kereszt A, Kevel Z, Mihacea S, Kalo P, Kiss G (2002) A receptor kinase gene regulating symbiotic nodule development. *Nature* 417: 962–966

- Forrest SI, Verma DPS, Dhindsa RS (1991) Starch content and activities of starch-metabolizing enzymes in effective and ineffective root nodules of soybean. *Can J Bot* **69**: 697–701
- Gadish I, Zamir D (1986) Differential zygotic abortion in an interspecific *Lycopersicon* cross. *Genome* **29**: 156–159
- Gage DJ, Bobo T, Long SR (1996) Use of green fluorescent protein to visualize the early events of symbiosis between *Rhizobium meliloti* and alfalfa (*Medicago sativa*). *J Bacteriol* **178**: 7159–7166
- Geurts R, Heidstra R, Hadri A-E, Downie JA, Franssen H, van Kammen A, Bisseling T (1997) Sym2 of pea is involved in a nodulation factor-perception mechanism that controls the infection process in the epidermis. *Plant Physiol* **115**: 351–359
- Guinel FC, Sloetjes LL (2000) Ethylene is involved in the nodulation phenotype of *Pisum sativum* R50 (*sym16*), a pleiotropic mutant that nodulates poorly and has pale green leaves. *J Exp Bot* **51**: 885–894
- Guinel FC, LaRue TA (1991) Light microscopy study of nodule initiation in *Pisum sativum* L. cv Sparkle and in its low-nodulating mutant E2 (*sym5*). *Plant Physiol* **97**: 1206–1211
- Handberg K, Stougaard J (1992) *Lotus japonicus*, an autogamous, diploid legume species for classical and molecular genetics. *Plant J* **2**: 487–496
- Hayashi M, Imaizumi-Anraku H, Akao S, Kawaguchi M (2000) Nodule organogenesis in *Lotus japonicus*. *J Plant Res* **113**: 489–495
- Herrmann B, Mattsson M, Fuhrer J, Schjoerring JK (2002) Leaf-atmosphere NH₃ exchange of white clover (*Trifolium repens* L.) in relation to mineral N nutrition and symbiotic N₂ fixation. *J Exp Bot* **53**: 139–146
- Imaizumi-Anraku H, Kawaguchi M, Koiwa H, Akao S, Syono K (1997) Two ineffective-nodulating mutants of *Lotus japonicus*: different phenotypes caused by the blockage of endocytic bacterial release and nodule maturation. *Plant Cell Physiol* **38**: 871–881
- Imaizumi-Anraku H, Kouchi H, Syono K, Akao S, Kawaguchi M (2000) Analysis of *ENOD40* expression in *alb1*, a symbiotic mutant of *Lotus japonicus* that forms empty nodules with incompletely developed nodule vascular bundles. *Mol Gen Genet* **264**: 402–410
- Jiang Q, Gresshoff PM (1997) Classical and molecular genetics of the model legume *Lotus japonicus*. *Mol Plant-Microbe Interact* **10**: 59–68
- Kawaguchi M, Imaizumi-Anraku H, Koiwa H, Niwa S, Ikuta A, Syono K, Akao S (2002) Root, root hair, and symbiotic mutants of the model legume *Lotus japonicus*. *Mol Plant-Microbe Interact* **15**: 17–26
- Kneen BE, Weeden NF, LaRue TA (1994) Non-nodulating mutants of *Pisum sativum* (L.) cv. Sparkle. *J Hered* **85**: 129–133
- Kouchi H, Hata S (1993) Isolation and characterization of novel nodulin cDNAs representing gene expressed at early stages of soybean nodule development. *Mol Gen Genet* **238**: 106–119
- Krusell L, Madsen LH, Sato S, Aubert G, Genua A, Szczyglowski K, Duc G, Kaneko T, Tabata S, de Bruijn F et al. (2002) Shoot control of root development and nodulation is mediated by a receptor-like kinase. *Nature* **420**: 422–426
- Lee KH, LaRue TA (1992) Pleiotropic effects of *sym-17¹*: A mutation in *Pisum sativum* L. cv Sparkle causes decreased nodulation, altered root and shoot growth, and increased ethylene production. *Plant Physiol* **100**: 1326–1333
- Nishimura R, Hayashi M, Wu GJ, Kouchi H, Imaizumi-Anraku H, Murakami Y, Kawasaki S, Akao S, Ohmori M, Nagasawa M et al. (2002a) HAR1 mediates systemic regulation of symbiotic nodule development. *Nature* **420**: 426–429
- Nishimura R, Ohmori M, Fujita H, Kawaguchi M (2002b) A *Lotus* basic leucine zipper protein with a RING-finger motif negatively regulates the developmental program of nodulation. *Proc Natl Acad Sci USA* **99**: 15206–15210
- Nishimura R, Ohmori M, Kawaguchi M (2002c) The novel symbiotic phenotype of enhanced-nodulating mutant of *Lotus japonicus*: *astray* mutant is an early nodulating mutant with wider nodulation zone. *Plant Cell Physiol* **43**: 853–859
- Novak K, Pesina K, Nebesarova J, Skrdleta V, Lisa L, Nasinec V (1995) Symbiotic tissue degradation pattern in the ineffective nodules of three nodulation mutants of pea (*Pisum sativum* L.). *Ann Bot* **76**: 303–313
- Penmetsa RV, Cook DR (1997) A legume ethylene-insensitive mutant hyperinfected by its rhizobial symbiont. *Science* **275**: 527–530
- Postma JG, Jager D, Jacobsen E, Feenstra WJ (1990) Studies on a non-fixing mutant of pea (*Pisum sativum* L.): I. Phenotypical description and bacteroid activity. *Plant Sci* **68**: 151–161
- Ringli C, Baumberger N, Diet A, Frey B, Keller B (2002) ACTIN2 is essential for bulge site selection and tip growth during root hair development of Arabidopsis. *Plant Physiol* **129**: 1464–1472
- Schauser L, Handberg K, Sandal N, Stiller J, Thykjaer T, Pajuelo E, Nielsen A, Stougaard J (1998) Symbiotic mutants deficient in nodule establishment identified after T-DNA transformation of *Lotus japonicus*. *Mol Gen Genet* **259**: 414–423
- Schauser L, Roussis A, Stiller J, Stougaard J (1999) A plant regulator controlling development of symbiotic root nodules. *Nature* **402**: 191–195
- Smith PMC, Winter H, Storer PJ, Bussell JD, Schuller KA, Atkins CA (2002) Effect of short-term N₂ deficiency on expression of the ureide pathway in cowpea root nodules. *Plant Physiol* **129**: 1216–1221
- Stracke S, Kistner C, Yoshida S, Mulder L, Sato S, Kaneko T, Tabata S, Sandal N, Stougaard J, Szczyglowski K et al. (2002) A plant receptor-like kinase required for both bacterial and fungal symbiosis. *Nature* **417**: 959–962
- Szczyglowski K, Shaw RS, Wopereis J, Copeland S, Hamburger D, Kasiborski B, Dazzo FB, de Bruijn FJ (1998) Nodule organogenesis and symbiotic mutants of the model legume *Lotus japonicus*. *Mol Plant-Microbe Interact* **11**: 684–697
- Tsyganov VE, Morzhina EV, Stefanov SY, Borisov AY, Lebsky VK, Tikhonovich IA (1998) The pea (*Pisum sativum* L.) genes *sym33* and *sym40* control infection thread formation and root nodule function. *Mol Gen Genet* **259**: 491–503
- Tsyganov VE, Voroshilova VA, Priefer UB, Borisov AY, Tikhonovich IA (2002) Genetic dissection of the initiation of the infection process and nodule tissue development in the *Rhizobium*-Pea (*Pisum sativum* L.) symbiosis. *Ann Bot* **89**: 357–366
- Vance CP, Johnson LEB (1983) Plant determined ineffective nodules in alfalfa (*Medicago sativa*): structural and biochemical comparisons. *Can J Bot* **61**: 93–106
- van Spronsen PC, Gronlund M, Bras CP, Spaik HP, Kijne JW (2001) Cell biological changes of outer cortical root cells in early determinate nodulation. *Mol Plant-Microbe Interact* **14**: 839–847
- Vasse J, de Billy F, Truchet G (1993) Abortion of infection during the *Rhizobium meliloti*-alfalfa symbiotic interaction is accompanied by a hypersensitive reaction. *Plant J* **4**: 555–566
- Walker SA, Downie JA (2000) Entry of *Rhizobium leguminosarum* bv. viciae into root hairs requires minimal Nod factor specificity, but subsequent infection thread growth requires *nodO* or *nodE*. *Mol Plant-Microbe Interact* **13**: 754–762
- Wopereis J, Pajuelo E, Dazzo FB, Jiang Q, Gresshoff PM, de Bruijn FJ, Stougaard J, Szczyglowski K (2000) Short root mutant of *Lotus japonicus* with a dramatically altered symbiotic phenotype. *Plant J* **23**: 97–114
- Xu Y, Zhu L, Xiao J, Huang N, McCouch SR (1997) Chromosomal regions associated with segregation distortion of molecular markers in F₂, backcross, double haploid, and recombinant inbred populations in rice (*Oryza sativa* L.). *Mol Gen Genet* **253**: 535–545
- Zamir D, Tadmor Y (1986) Unequal segregation of nuclear genes in plants. *Bot Gaz* **147**: 355–358